Breast Cancer (2016) 23:491–498
DOI 10.1007/s12282-015-0592-0

ORIGINAL ARTICLE

Histopathological characteristics of breast ductal carcinoma in situ and association with imaging findings

XiaoYan Tang · Tomohiro Yamashita · Makiko Hara · Nobue Kumaki · Yutaka Tokuda · Shinobu Masuda

Received: 26 August 2014 / Accepted: 25 January 2015 / Published online: 3 February 2015

Abstract
Background The treatment policy for ductal cancer in situ (DCIS) of the breast greatly depends on the spreading diagnosis. However, a problem is that we cannot compare imaging findings with the histopathology of DCIS. The purpose of this study was to investigate the histopathological characteristics of DCIS and the association with imaging findings.
Method Subjects were 185 patients from Tokai University Hospital, diagnosed with DCIS from April 2005 to December 2010. A positive finding on ultrasonography was defined as Breast Imaging Reporting and Data System (BI-RADS) of US category 3 or above, in mammography it was Japan Breast Cancer Society category 2 or above, and in MRI it was BI-RADS-MRI category 3 or above. Histopathologically, we re-classified flat and/or low papillary DCIS into type 1; papillary and/or cribriform DCIS into type 2; and comedo and/or solid DCIS into type 3.
Results The clinical characteristics and association between imaging findings and histopathological classification of the 3 subtypes of DCIS are summarized as follows: (1) histopathologically, in type 3, there was a higher frequency of necrosis and calcification in the ducts of DCIS (χ^2, $p < 0.001$), the number of dilated periductal capillaries was greater than in type 1 ($p = 0.023$), and the distribution of DCIS was concentrated in type 3 ($p = 0.020$); (2) on ultrasonography, type 3 was easier to detect than type 1 ($p = 0.008$); (3) on mammography and MRI, there were no significant differences between type 1 and type 3. The histopathological characteristics of small (<10 mm) DCIS and DCIS that cannot be detected by ultrasonography or MRI were also discussed.
Conclusion When carrying out spreading diagnosis of DCIS, we need to keep the histopathological type in mind and interpret the imaging findings comprehensively.

Keywords Breast · Ductal carcinoma in situ (DCIS) · Histopathology · Imaging findings

X. Tang (✉) · S. Masuda
Department of Pathology, Nihon University School of Medicine, 30-1 Oyaguchi-Kamicho, Itabashi-Ku, Tokyo 173-8610, Japan
e-mail: tang.xiaoyan@nihon-u.ac.jp

T. Yamashita
Department of Diagnostic Radiology, Tokai University, School of Medicine, Isehara, Kanagawa, Japan

M. Hara
Department of Clinical Laboratory, Urasoe General Hospital, Urasoe, Okinawa, Japan

N. Kumaki
Department of Pathology, Tokai University School of Medicine, Isehara, Kanagawa, Japan

Y. Tokuda
Department of Breast and Endocrine Surgery, Tokai University School of Medicine, Isehara, Kanagawa, Japan

Introduction

The concept of ductal carcinoma in situ of the breast (DCIS) was first established by Cheatle and Cutler [1] and Muir [2] quantitatively. The incidence of DCIS rose from 1 to 20–30 % [3] in the USA, primarily due to invention and the widespread use of mammography examination, in the early 1990s. The Japanese Breast Cancer Society published statistical data in 2011 and reported that the incidence of DCIS in Japan female breast cancer was 14.2 % [4].

On the classification of DCIS, it has long been generally accepted that there are 6 subtypes, which were proposed by Rosen [5, 6] based on the morphology, and in most cases DCIS showed a mix of several subtypes with one or two major subtypes. DCIS may also be graded and classified based on the nuclear atypia and architecture of DCIS cells, as well as presence/absence of necrosis [7]. The WHO classification of tumors of the breast divides DCIS into 3 grades, low, intermediate, and high [8]. Silverstein et al. [9] developed a van Nuys classification system of DCIS based on nuclear atypia and comedo necrosis. This system also showed a significant correlation with local recurrence and disease-free survival, so it is widely used. Silverstein et al. [10] established the van Nuys Prognostic Index (VNPI) systems and, in 2003, the USC/VNPI system, and used the histopathological types of DCIS, tumor size, state of the surgical margin, and patient's age to guide treatment choices [11]. However, the report did not summarize the correlation between the histopathological subtypes and imaging diagnoses. For pathologists, it is difficult to categorize DCIS diagnoses in breast cancer, especially with needle biopsy materials. However, imaging findings of ultrasonography, mammography, and magnetic resonance imaging (MRI) may be helpful for histological diagnosis. Therefore, the purpose of this study was to identify the histopathological characteristics of DCIS that correspond with imaging findings.

Patients and methods

We selected 185 DCIS patients, who were diagnosed with DCIS histopathologically (including 17 patients with DCIS with microinvasion) from April 2005 to December 2010 in Tokai University Hospital. All patients were female, aged 25–81 years. All patients consented to modified mastectomy or partial resection of the breast. We re-classified 128 of the 185 patients with DCIS, who underwent both ultrasonography and mammography, into 3 types. Of these, 102 underwent MRI examination. We re-classified flat and/or low papillary DCIS into type 1; papillary and/or cribriform DCIS into type 2; and comedo and/or solid DCIS into type 3. Our re-classification was based on the following. (1) as we know, ultrasonic images are created by sending a pulse of ultrasound into the tissue, and ultrasonography involves recording the sound reflected from parts of the tissue. The density and uniformity, in histopathologic terms, the cellularity (the amount of cell components in ducts) and proportion (arranged structures of cells) of the tissue, directly influence the ultrasonic level of B-mode imaging. So, we focused on the cellularity in the ducts of DCIS. Mammography imaging is also affected by the "tissue density", and X-rays are absorbed when they pass through the tissue. However, MRI was not taken into consideration. (2) According to the 6 subtypes proposed by Rosen [5, 6], the structure of DCIS can be classified as flat, micropapillary, papillary, cribriform, solid, and comedo. In most cases, DCIS showed a mix of several subtypes with one or two major subtypes. Flat-type DCIS was sometimes described as "clinging" and often combined with micropapillary DCIS. Both these types have less cell components in the ducts, so we re-classified these into type 1. Most of the solid and comedo-type DCISs show high nuclear grade and colocalization. They also show the highest cellularity in the ducts, and so we re-classified those two types into type 3. Usually, micropapillary DCIS progresses into cribriform DCIS, but papillary DCIS can also form cribriform structures [6]. The cellularity of cribriform and papillary DCIS is positioned between types 1 and 3, and so we classed these as type 2. However, solid papillary-type DCIS was classed as type 3.

Histopathological re-classification is summarized in Table 1 and Fig. 1, and the clinical characteristics of our cases are summarized in Table 2.

The microscopic examination items included the nuclear grade of carcinoma cells, necrosis and calcification in the DCIS lumina, stromal reactions surrounding DCIS ducts, distribution of DCIS, and presence or absence of adenosis or other benign changes in the background breast. Examination items were selected mainly according to the principle of ultrasonography mentioned above; for example, ultrasound energy passes through fluid easily with minimal loss, so stromal reaction including edematous or myxoid change was discussed. Fibrosis was selected as a comprehensive item of elastosis and irregular sclerotic change in the periductal region of DCIS. One maximum cut slide of the tumor was examined. The nuclear grade was justified according to the general rules for the clinical and pathological recording of breast cancer (17th edition). Necrosis and calcification were determined when necrotic and calcifying changes were observed in one DCIS duct, and secretory or necrotic calcification did not differ. Stromal

Table 1 Histopathological classification of the 3 DCIS subtypes in this study

Subtypes	Architectures of DCIS
Type 1	Flat and/or micropapillary (low papillary)
Type 2	Cribriform and/or papillary
Type 3	Solid and/or comedo, solid or comedo with any other architecture patterns, e.g.; solid and cribriform or papillary or micropapillary or flat, comedo and cribriform or papillary or micropapillary or flat, and solid-papillary, etc.

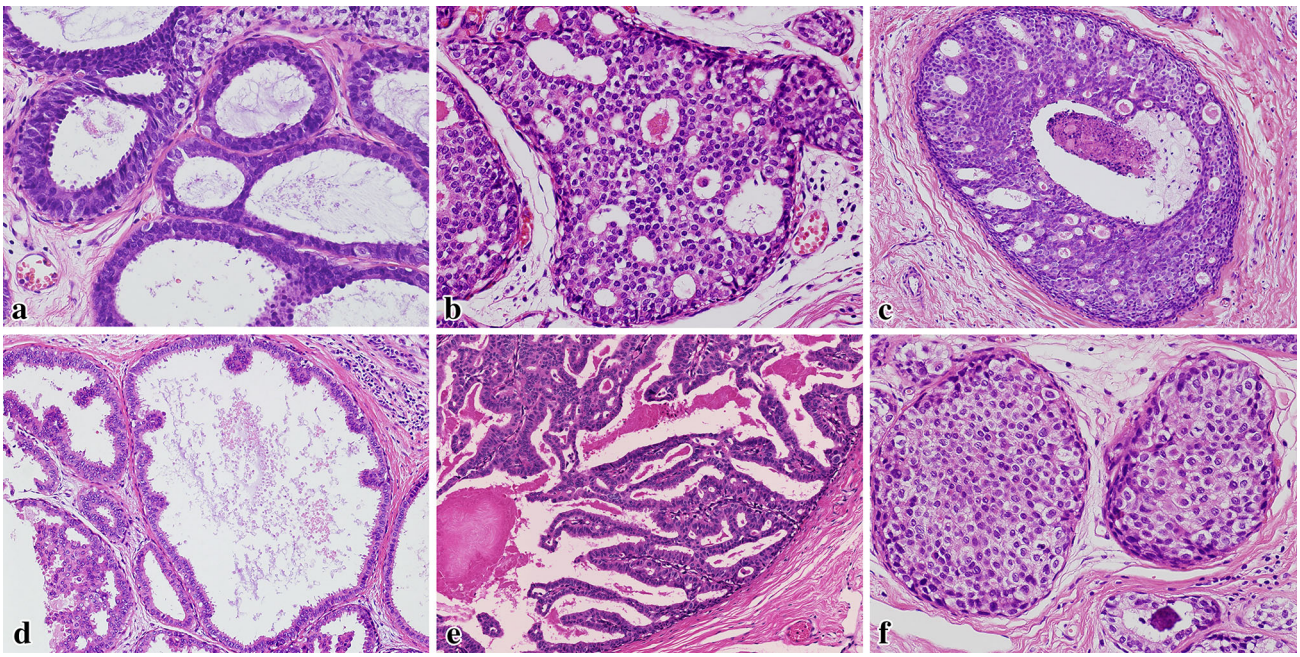

Fig. 1 Histopathological classification of the 3 DCIS subtypes in this study. **a**, **d** Flat and low papillary types were referred to as type 1 DCIS; **b**, **e** cribriform and papillary types were referred to as type 2 DCIS; **c**, **f** comedo and solid types were referred to as type 3 DCIS

reactions, including inflammatory cell infiltration, fibrosis, edematous or myxoid change, and increasing and/or dilatation of periductal capillaries, and the distribution of DCIS were not measured digitally and a subjective judgment was determined by a pathologist.

Ultrasonography, mammography, and MRI were performed routinely using Aplio XG SSA-770A or 790A scanners with a 12-MHz linear imaging transducer (PLT-1204BT) (Toshiba Medical Imaging Systems), Lorad-M IV Unit (Lorad Medical Systems-Hologic), and Achieva 3.0 TX (Philips Medical System), and imaging findings were extracted. The MRI findings were from one radiologist, and the mammography findings were also reviewed by the same radiologist when he judged the MR image. The ultrasonography findings were interpreted by specialists. This is because this examination provides images in real time and so reviewing of the image is almost impossible. However, all images of our cases were routinely discussed at a clinical pathology conference (CPC), and the findings of ultrasonography were also confirmed by CPC members.

The guidelines edited by the Japan Association of Breast and Thyroid Sinology (JABTS), Japan Radiological Society (JRS), Japan Association of Breast Cancer Screening (JABCS), and Japan Breast Cancer Society (JBCS) were used in routine examination and to define positive findings. The category systems of Breast Imaging Reporting and Data System (BI-RADS)-US and BI-RADS-MRI devised by the American College of Radiology (ACR) were also used. A positive finding on ultrasonography was defined as BI-RADS-US category 3 or above, in mammography it was JBCS category 2 or above, and in MRI it was BI-RADS-US category 3 or above. The association between clinical and histopathological characteristics of the 3 subtypes of DCIS and imaging findings were discussed. For statistical analysis, the χ^2 test was performed using IBM SPSS statistics 19, and the results were significant when $p < 0.05$.

Results

The most frequent presentation in our patients ($n = 185$) was abnormal mammography findings after a screening examination (61.08 %), a palpable mass found out by the patient herself (20.00 %), nipple discharge (8.64 %), abnormal findings on ultrasonography screening (5.94 %), and unknown (4.32 %). However, no significant differences in the presentation or age at onset were identified in the 3 subtypes.

In 114 cases found to be positive on ultrasonography, 33 mass lesions, 6 mass with dilated duct lesions, 69 hypoechoic non-mass lesions, and 11 cystic lesions were included and overlap was present. In 13 mammography category 2 (C2) cases, there were 12 calcifications and 1 mass lesion; in 101 cases above C2, 9 mass lesions, 66 calcifications, 10 distortions, and 7 FAD lesions were identified. In 96 cases found to be positive on MRI, 25

Table 2 Relationship between clinical and histopathological characteristics of the 3 subtypes of DCIS and imaging findings ($n = 128$)

DCIS subtype	Type 1 ($n = 15$)	Type 2 ($n = 33$)	Type 3 ($n = 80$)	p
Nuclear grade				0.109
Grade 1	5 (33.33 %)	10 (30.30 %)	22 (27.50 %)	
Grade 2	8 (53.33 %)	22 (66.66 %)	38 (47.50 %)	
Grade 3	2 (13.33 %)	1 (3.03 %)	20 (25.00 %)	
Necrosis/calcification				0.000
−/−	3 (20.00 %)	16 (48.48 %)	19 (23.75 %)	
−/+	7 (46.67 %)	8 (24.24 %)	8 (10.00 %)	
+/−	3 (20.00 %)	4 (12.12 %)	9 (11.25 %)	
+/+	2 (13.33 %)	5 (15.15 %)	44 (55.00 %)	
Stromal reaction				
Inflammatory cell infiltration				0.230
+	8 (53.33 %)	12 (36.36 %)	43 (53.75 %)	
−	7 (46.67 %)	21 (63.63 %)	37 (46.25 %)	
Edematous and/or myxoid changes				0.183
+	7 (46.67 %)	15 (45.45 %)	50 (62.50 %)	
−	8 (53.33 %)	18 (54.55 %)	30 (37.50 %)	
Fibrosis				0.799
+	5 (33.33 %)	8 (24.24 %)	21 (26.25 %)	
−	10 (66.67 %)	25 (75.76 %)	59 (73.75 %)	
Periductal capillaries				0.023
+	10 (66.67 %)	24 (72.73 %)	67 (83.75 %)	
−	5 (33.33 %)	9 (27.27 %)	13 (16.25 %)	
DCIS distribution				0.020
Concentrated	4 (26.67 %)	23 (69.70 %)	33 (41.25 %)	
Scattered	11 (73.33 %)	10 (30.30 %)	47 (58.75 %)	
Adenosis				0.355
+	4 (26.67 %)	9 (27.27 %)	15 (17.50 %)	
−	11 (73.33 %)	24 (72.73 %)	66 (82.50 %)	
Findings on US				0.008
+	10 (66.67 %)	29 (87.88 %)	75 (93.75 %)	
−	5 (33.33 %)	4 (12.12 %)	5 (6.26 %)	
Findings on MMG				0.763
+	14 (93.33 %)	31 (93.94 %)	72 (90.00 %)	
Calcification present cases	12 (85.71 %)	19 (61.29 %)	52 (65.00 %)	
−	1 (6.67 %)	2 (6.06 %)	8 (10.00 %)	
Findings on MRI				0.192
+	12 (85.71 %)	24 (100 %)	60 (93.75 %)	
−	2 (14.29 %)	0	4 (6.25 %)	
Not administered	1	9	16	

DCIS ductal carcinoma in situ, *US* ultrasonography, *MMG* mammography, the results were significant when $p < 0.05$

showed a mass lesion and 71 showed segmental or ductal pattern enhancement of lesions.

Histopathologically, no differences in the nuclear grade could be identified between the 3 subtypes, but there was a higher frequency of necrosis and calcification in type 3 DCIS ducts ($p < 0.001$). Regarding the stromal reaction, inflammatory cell infiltration, edematous or myxoid change, and fibrosis were observed without peculiarity in all 3 subtypes. In type 3 DCIS, increasing and dilatation of periductal capillaries was often seen ($p = 0.023$), and the distribution of DCIS ducts was more concentrated in type 3 than in type 1 ($p = 0.020$). The occurrence of adenosis or similar benign changes in the background breast did not correlate with the subtype classification. In imaging findings, type 3 was easier to detect than type 1 on ultrasonography ($p = 0.008$), but there were no significant differences in mammography and MRI. No patient with type 1 DCIS had been diagnosed by ultrasonography screening. However, 66.67 % of type 1 lesions could be detected by ultrasonography when we conducted a second

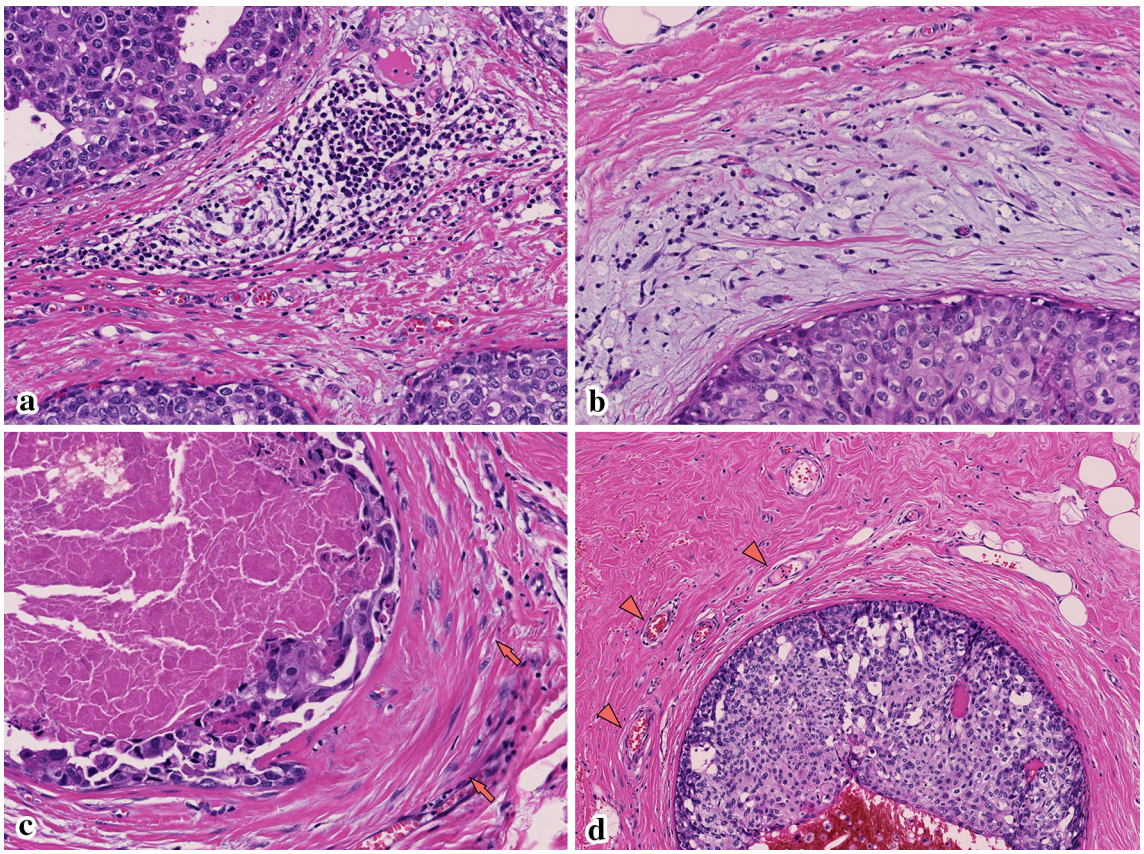

Fig. 2 Stromal changes surrounding DCIS ducts. **a** Inflammatory cell infiltration in the stroma; **b** edematous and myxoid change of the stroma surrounding the DCIS duct; **c** fibrosis with increased collagen fibers in the stroma (*red arrow*); **d** increased number of dilated periductal capillaries (*red arrowhead*) (color figure online)

look examination. This rate was much lower than in type 2 (87.88 %) and type 3 (93.75 %). This indicates that types 2 and 3 were easier to detect than type 1 by ultrasonography ($p = 0.008$), and the examination also correlated with the technique and intention of the practitioner. The associations between clinical and histopathological characteristics of the 3 subtypes of DCIS and imaging findings are summarized in Table 2. The stromal changes are shown in Fig. 2.

We also summarized the characteristics of 12 small (<10 mm) DCIS cases, based on histopathological subtypes, nuclear grades, necrosis and calcification, stromal reactions, distribution of DCIS, presence or absence of adenosis or other benign changes in the non-neoplastic breast, and correlation with MMG and MRI findings. The tumor size was measured using a mapping figure made by pathologists. Compared to 96 large size cases (>10 mm), small cases showed less inflammatory cell infiltration ($p = 0.011$) or edematous or myxoid change ($p = 0.047$) in the stroma and more concentrated DCIS ducts ($p = 0.010$), but were less likely to be detected by MRI ($p = 0.034$). The 3 subtype DCIS classifications, nuclear grade, and other parameters showed no significant differences.

In the 14 DCIS cases that could not be detected by ultrasonography, the same items were analyzed. Three of the 14 cases were <10 mm, and 11 of the 14 were >10 mm ($p = 0.148$). Compared to the 115 detected cases, these 14 undetected cases showed slight edematous or myxoid change in the stroma histopathologically ($p < 0.001$) and were less likely to be detected by MRI ($p = 0.004$). In 6 MRI undetected cases, 2 were <10 mm, 3 were >10 mm, and 1 had an unknown size; they were less likely to be detected by ultrasonography ($p = 0.004$), and the occurrence of adenosis or other benign changes in the background breast interfered with MRI ($p = 0.010$). Periductal capillaries seemed to be an important factor for MRI detection ($p = 0.007$). No other histopathological differences in the 3 subtype DCIS classifications, nuclear grade, etc. could be found. However, all "undetected cases" were detected by mammography examination.

Discussion

We described the histopathological characteristics of DCIS and the association with imaging diagnosis.

Ultrasonography is useful and the most frequently used method for breast cancer diagnosis. It was indicated that ultrasonography detection was correlated with the histological grade when using the van Nuys classification system [12]. Our study also showed that myxoid change of the stroma surrounding DCIS ducts was favorable for ultrasonography, and the DCIS ducts should be concentrated enough to be detected, especially for small DCIS lesions (Fig. 3). Cases difficult to detect by ultrasonography were also difficult to detect by MRI, but could be identified by MMG in many cases, particularly with calcification.

Microcalcification is one of the most important findings of DCIS on mammography. Calcium can deposit both on necrotic debris (necrotic calcification) and non-necrotic materials, such as secretory or mucinous materials (non-necrotic calcification) [12, 13]. Most of the time, the non-necrotic (secretory) calcifications are round and punctate, or fine granular and amorphous microcalcifications, while necrotic calcifications are considered to be irregular, pleomorphic, and coarse heterogenous microcalcifications on mammography [14]. Histopathologically, necrosis and calcification was less frequently observed in type 1 than type 3 ($p < 0.001$). In necrosis (−)/calcification (+) cases, type 1 comprised 46.67 %, while type 3 comprised 10.00 %. On the other hand, in showing necrosis (+)/calcification (+), type 1 comprised 13.33 %, and type 3 comprised 80.00 %. This means that type 3 DCIS usually shows irregular, pleomorphic, and coarse heterogenous microcalcifications, and type 1 DCIS is often observed as round and punctate, or thin and amorphous microcalcifications on mammography.

MRI was sensitive for all 3 subtypes of DCIS, but its sensitivity was poor for smallness lesions in this study. It is known that some benign diseases of the breast, such as mastopathy (adenosis), fibrosis, or mastitis, also show enhancement on contrast-enhanced MRI [15]. Our study indicated that adenosis or other benign changes of the breast increased the difficulty of DCIS detection ($p = 0.010$). It was previously reported that the so-called clustered ring enhancement on MRI reflected an intraductal carcinoma with an abundant blood supply and the contrast medium that accumulated in the periductal stroma or ductal wall [16]. Our study revealed that the periductal capillaries showed a close association with MRI detection, and abundant dilated capillaries may sometimes overcome the disturbance from the coexistence of adenosis or other benign changes (Fig. 4). On comparison with mammography, MRI showed favorable sensitivity for DCIS of low nuclear grade (WHO classification), and it was

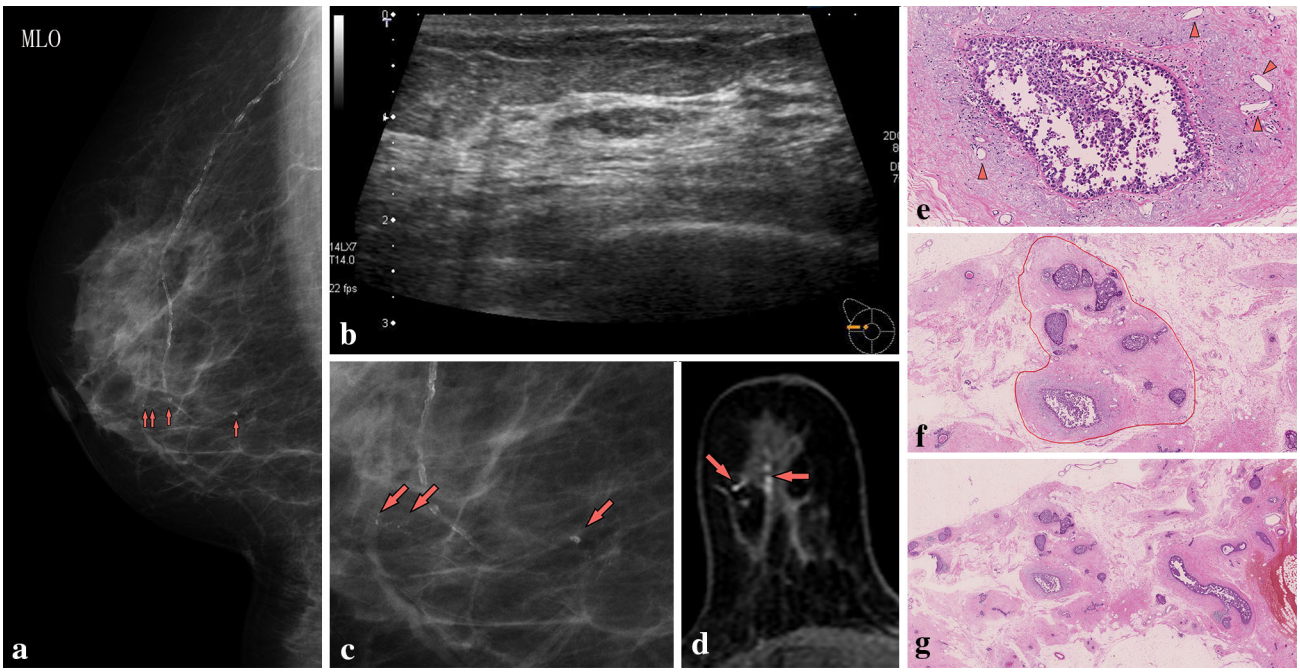

Fig. 3 The case was a 74-year-old female with microcalcification (*red arrow*) on screening mammography [mediolateral oblique (MLO)] (**a**, **c**), a hypoechoic non-mass lesion on ultrasonography (**b**), and multiple clumped enhancements on contrast-enhanced MRI (*red arrow*, sagittal plane) (**d**). The pathologic diagnosis was a DCIS lesion, at 9 × 3 mm. The DCIS cells showed a solid to papillary architecture (**e** and **f**), and DCIS ducts were scattered (**g**). The stroma surrounding the DCIS ducts showed marked edematous and myxoid change accompanied by dilated capillaries (*red arrowhead)* (**e**). This adenomatous and myxoid change led to several single DCIS ducts being "confused" as a big "solid unit" (*surrounded by red line*) (**f**), and these features were presumed to improve detection by ultrasonography and MRI (color figure online)

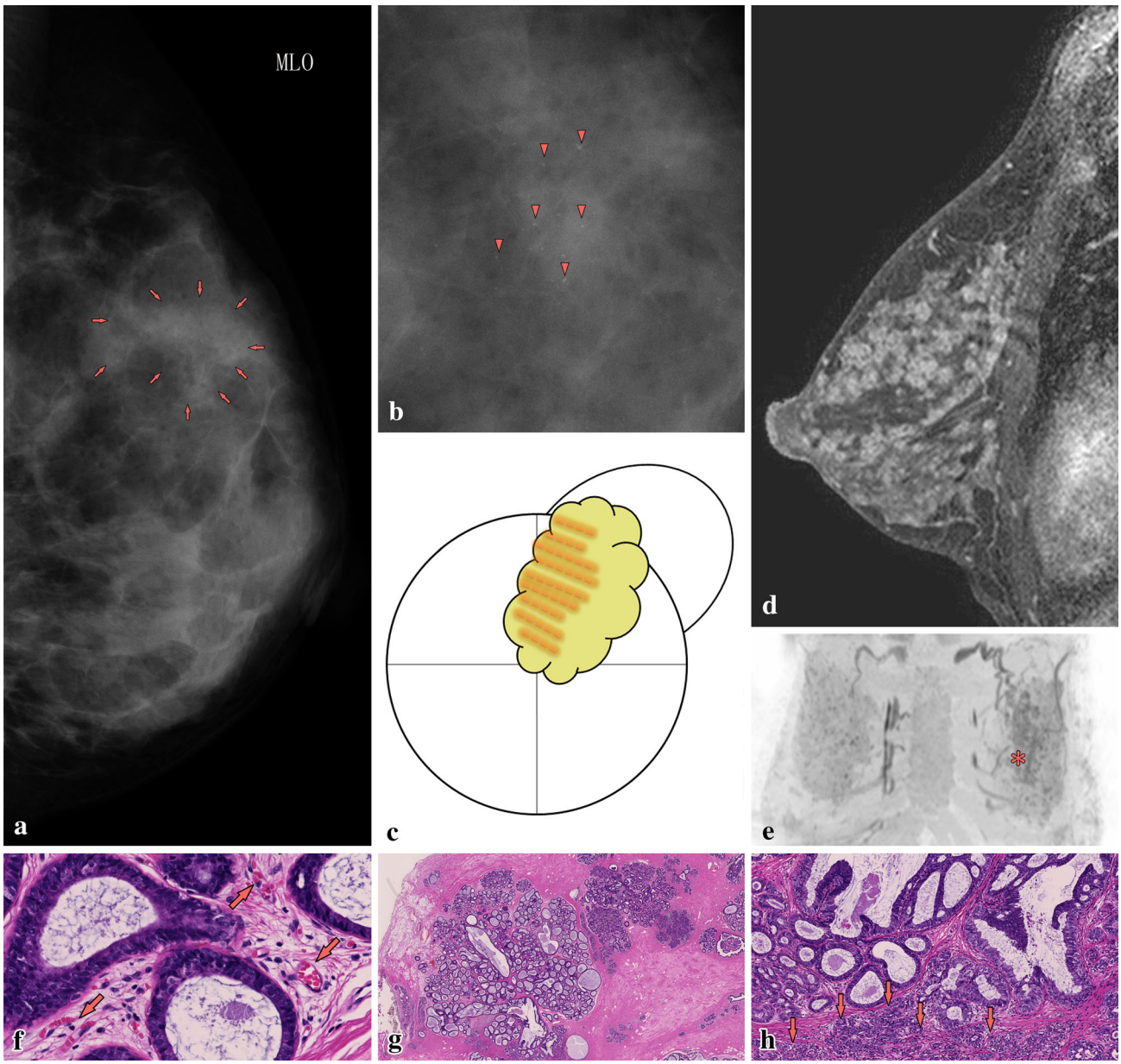

Fig. 4 The case was a 42-year-old female with punctuate or amorphous microcalcifications on screening mammography [**a**, **b**, *red arrow* and *red arrowhead*, mediolateral oblique (MLO)]. MRI revealed periductal enhancement (clustered ring enhancement, horizontal plane), and DCIS was strongly suspected (**d**). DCIS was mapped on the partially resected breast sample (**c**, the *orange line* indicated DCIS), and the spreading area was matched to the MIP feature of MRI (**e**, *asterisk* indicated nipple). Dilated capillaries (*red arrow*) were identified surrounding DCIS ducts (**f**). Histopathologically, this was a type 1 DCIS (**f** and **h**) case accompanied by frequent adenosis (**h**, *red arrow*) in the background breast, and capillaries probably promoted the enhancement of DCIS on MRI. The adenosis area involving DCIS (*left big cluster*) was prominently enlarged than the adenosis area (*right small clusters*) (**g**) (color figure online)

recommended that MRI can improve the ability to diagnose DCIS, especially DCIS with a high nuclear grade [17]. In this study, however, we did not identify a difference between the 3 histopathological subtypes on MRI.

In conclusion, ultrasonography imaging reflected the histopathological classification of DCIS, myxoid changes of the stroma surrounding DCIS and the concentration of DCIS ducts. MRI was correlated with the periductal capillaries of DCIS and adenosis changes in the background breast, while mammography can make up for the shortcomings of ultrasonography and MRI. It is important for us to refer to imaging diagnosis and histopathological findings when we do a spreading diagnosis of DCIS and a comprehensive judgment is necessary.

Acknowledgments This work was supported by a Grant for "Strategic Research Base Development" Program for Private Universities subsidized by MEXT (2010).

Conflict of interest Yutaka Tokuda received research funding from Chugai Pharmaceutical Co., Ltd, Taiho Pharmaceutical Co., Ltd, Takeda Pharmaceutical Co., Ltd, and Novartis Pharma K.K. The other authors declare that there are no conflicts of interest.

References

1. Cheatle GL, Cutler M. Malignant epithelial neoplasia. Carcinoma. The precancerous or potentially carcinomatous state. In: Cheatle GL, Cutler M, editors. Tumours of the breast. 1st ed. Philadelphia: Lippincott; 1926. p. 161–332.
2. Muir R. The intra-epithelial growth of carcinoma. Br Med J. 1930;11:587–9.
3. Kumar AS, Bhatia V, Henderson IC. Overdiagnosis and overtreatment of breast cancer. Rates of ductal carcinoma in situ: a US perspective. Breast Cancer Res. 2005;7:271–5.
4. The report of clinical statistical studies on registered mammary cancer patients in Japan. No. 42, (2011) The Japanese breast cancer society (JBCA) register. http://www.jbcs.gr.jp. Accessed 31 May 2014.
5. Rosen PP. Intraductal carcinoma. In: Rosen PP, editor. Rosen's breast pathology. 3rd ed. Philadelphia: Lippincott Williams & Wilkins; 2009. p. 291–341.
6. Rosen PP. Papillary carcinoma. In: Rosen PP, editor. Rosen's breast pathology. 3rd ed. Philadelphia: Lippincott Williams & Wilkins; 2009. p. 423–48.
7. Allred DC. Ductal carcinoma in situ: terminology, classification, and natural history. J Natl Cancer Inst Monogr. 2010;41:134–8.
8. Schnitt SJ, Allred C, Britton P, Ellis IO, Lakhani SR, Morrow M. Ductal carcinoma in situ. In: Lakhani SR, Ellis IO, Schnitt SJ, Tan PH, van de Vijver MJ, editors. WHO classification of tumours of the breast. 4th ed. Lyon: IARC press; 2012. p. 90–4.
9. Silverstein MJ, Poller DN, Waisman JR, Colburn WJ, Barth A, Gierson ED, et al. Prognostic classification of breast ductal carcinoma-in-situ. Lancet. 1995;345:1154–7.
10. Silverstein MJ, Laqios MD, Craig PH, Waisman JR, Lewinsky BS, Colburn WJ, et al. A prognostic index for ductal carcinoma in situ of the breast. Cancer. 1996;77:2267–74.
11. Silverstein MJ. The University of Southern California/Van Nuys prognostic index for ductal carcinoma in situ of the breast. Am J Surg. 2003;186:337–43.
12. Gwak YJ, Kim HJ, Kwak JY, Lee SK, Shin KM, Lee HJ, et al. Ultrasonographic detection and characterization of asymptomatic ductal carcinoma in situ with histopathologic correlation. Acta Radiol. 2011;52:364–71. doi:10.1258/ar.2011.100391.
13. Tse GM, Tan PH, Cheung HS, Chu WC, Lam WW. Intermediate to highly suspicious calcification in breast lesions: a radio-pathologic correlation. Breast Cancer Res Treat. 2008;110:1–7. doi:10.1007/s10549-007-9695-4.
14. Tse GM, Tan PH, Pang ALM, Tang APY, Cheung HS. Calcification in breast lesions: pathologists' perspective. J Clin Pathol. 2008;61:145–51. doi:10.1136/jcp.2006.046201.
15. Sotome K, Yamamoto Y, Hirano A, Takahara T, Hasegawa S, Nakamaru M, et al. The role of contrast enhanced MRI in the diagnosis of non-mass image-forming lesions on breast ultrasonography. Breast Cancer. 2007;14:371–80.
16. Tozaki M, Igarashi T, Fukuda K. Breast MRI using the VIBE sequence: clustered ring enhancement in the differential diagnosis of lesions showing non-masslike enhancement. AJR. 2006;187:313–21.
17. Kuhl CK, Schrading S, Bieling HB, Wardelmann E, Leutner CC, Koenig R, et al. MRI for diagnosis of pure ductal carcinoma in situ: a prospective observational study. Lancet. 2007;370:485–92.